Combined electrocoagulation and electro-oxidation of industrial textile wastewater treatment in a continuous multi-stage reactor

Edison GilPavas, Paula Arbeláez-Castaño, José Medina and Diego A. Acosta

ABSTRACT

A combined electrocoagulation (EC) and electrochemical oxidation (EO) industrial textile wastewater treatment potential is evaluated in this work. A fractional factorial design of experiment showed that EC current density, followed by pH, were the most significant factors. Conductivity and number of electrooxidation cells did not affect chemical oxygen demand degradation (DCOD). Aluminum and iron anodes performed similarly as sacrificial anodes. Current density, pH and conductivity were chosen for a Box–Behnken design of experiment to determine optimal conditions to achieve a high DCOD minimizing operating cost (OC). The optimum to achieve a 70% DCOD with an OC of USD 1.47/m^3 was: pH of 4, a conductivity of 3.7 mS/cm and a current density of 4.1 mA/cm^2. This study also shows the applicability of a combined EC/EO treatment process of a real complex industrial wastewater.

Key words | electrochemical advanced oxidation processes, electrocoagulation, electro-oxidation, industrial textile wastewater, optimization

Edison GilPavas (corresponding author)
Paula Arbeláez-Castaño
José Medina
Departamento de Ingeniería de Procesos, GIPAB: Grupo de Investigación en Procesos Ambientales,
Universidad EAFIT,
Carrera 49 No. 7 sur 50,
Medellín,
Colombia
E-mail: egil@eafit.edu.co

Diego A. Acosta
Departamento de Ingeniería de Procesos. DDP: Grupo de investigación de Desarrollo y Diseño de Procesos,
Universidad EAFIT,
Carrera 49 No. 7 sur-50,
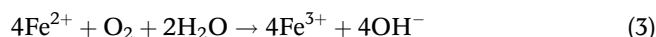Medellín,
Colombia

INTRODUCTION

Currently, industrial textile wastewater (TWW) treatment, a complex process, is the focus of research. In textile manufacturing processes, different dyes and auxiliary products (e.g. organic acids, fixing agents, reducing agents, and oxidizing agents) are released into residual waters (Soares *et al.* 2017). The resulting effluents are a major environmental problem if not properly treated before discharging them into water bodies or municipal wastewater treatment facilities (Alinsafi *et al.* 2005). TWW has intense color, high organic compounds concentration (i.e. chemical oxygen demand (COD) ranging from 200 to 3,000 mg/L) (Phalakornkule *et al.* 2010), low biodegradability ratio (i.e. BOD$_5$/COD ratio < 0.35) (Ghanbari & Moradi 2015) and a large amount of total suspended and dissolved solids (Verma *et al.* 2012).

Different approaches proven to be effective in the reduction of color and COD have been made to address TWW treatment: coagulation/flocculation (Verma *et al.* 2012), electrochemical coagulation (Tezcan & Aytac 2013), Fenton processes (Sreeja & Sosamony 2016), electrochemical oxidation (EO) (Moreira *et al.* 2017) and peroxi-coagulation (Ghanbari & Moradi 2015). However,

every method has shortcomings: (i) ozonization is efficient for color removal but inefficient for COD reduction; (ii) chemical and electrochemical coagulation processes are useful to completely remove suspended solids, but not highly soluble organic compounds (Verma *et al.* 2012). To overcome the limitations of a single-stage treatment of TWW, multi-stage treatments have been proposed to achieve higher pollutant elimination efficiencies. The combination of chemical and electrochemical coagulation with advanced oxidation process (AOPs) has been addressed and proven to be highly efficient to treat diverse wastewaters (sugar cane distillery (Rodrigues *et al.* 2017), landfills (Amor *et al.* 2015), textile (GilPavas *et al.* 2017). To the best of our knowledge, a combined TWW treatment by electrocoagulation (EC) and EO in a multistage continuous reactor has not been reported.

In the combined TWW treatment, EC uses a sacrificial anode that, when subject to electric current in-situ, releases metal cations that destabilize and aggregate particles into a floc of metallic hydroxides and polyhydroxides (Alinsafi

et al. 2005). Simultaneously, H_2 bubbles are formed in the cathode that induce sludge flotation. EC removes the smallest colloidal particles, as opposed to traditional flocculation and coagulation, and generates small amounts of sludge (Gatsios *et al.* 2015). This method has been successfully applied to treat various industrial wastewaters (Gatsios *et al.* 2015; Moussa *et al.* 2017). Generally, iron or aluminum electrodes are used for EC due to their low cost, availability, and formation of mainly amorphous metal oxides/hydroxides/oxyhydroxides with excellent adsorption properties of soluble species. Metal oxidation at the anode is described by Equation (1), where Z is the number of electrons transferred in the anodic dissolution process. Equations (2) and (3) describe the hydroxide formation from Al and Fe metal ions. EC's mechanism has been described (Hakizimana *et al.* 2017).

$$M \rightarrow M^{Z+} + Ze^- \tag{1}$$

$$Al^{3+} + H_2O \rightarrow AlOH^{2+} + H^+ \tag{2}$$

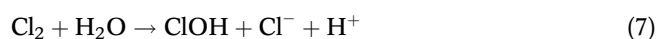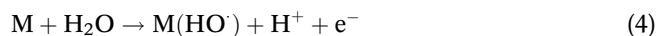$$4Fe^{2+} + O_2 + 2H_2O \rightarrow 4Fe^{3+} + 4OH^- \tag{3}$$

TWW treatment at bench scale experiments by EC has been done, but industrial employment of EC has not received much attention. However, this method is becoming popular because of its environmental compatibility, versatility, energy efficiency, safety, selectivity, amenability to automation and cost effectiveness (Moussa *et al.* 2017). The efficiency of EO is highly dependent on pollutants' mass transfer from the bulk to the anode surface or its vicinity. Two very distinct behaviors of organic pollutants degradation, depending on the anode material (AM), have been reported: (i) partial organics DCOD, along with the formation of many refractory species as final products, and (ii) large or total organics mineralization, i.e., conversion into CO_2, water and inorganic ions, together with the production of few or nil amounts of refractory intermediates.

Subsequent EO produces reactive oxygen species to oxidize the remaining organic pollutants resistant to EC destabilization. EO's main decontamination pathway consists of pollutant oxidation by a chemical reaction with electrogenerated hydroxyl radicals ($^\cdot$OH) from water discharge at the anode M such as chemisorbed 'active oxygen' (oxygen in the lattice of a metal oxide anode MO) or physically adsorbed 'active oxygen' (physisorbed

$M(^\cdot OH)$) (Brillas & Martínez-Huitle 2015). Carbonaceous materials such as graphite have been widely used in EO due to their great working potential window, low cost, low density, large surface area, compressibility, high electrical conductivity and good electron transport capacity. Also, graphite can bear very high current density, is chemically inert and has low resistivity. In addition, graphite was used as the anode because O_2 overpotential is high on graphite while Cl_2 overpotential is low, so this would increase current efficiency of Cl_2 evolution.

Graphite anodes also generate active chlorine when Cl^- species are present. Equations (4)–(7) explain the mechanism of $^\cdot$OH radical formation and chlorine species DCOD. Water may be oxidized, and leads to formation of hydronium cations and oxygen gas (Equation (5)), and in the presence of chloride anions, Cl^- may be oxidized into Cl_2 (Equation (6)). The latter, being a strong oxidant, may contribute to the oxidation of dissolved organic compounds or may lead to the formation of ClOH (Equation (7)), which also plays the role of oxidant (Kariyajjanavar *et al.* 2013).

$$M + H_2O \rightarrow M(HO^\cdot) + H^+ + e^- \tag{4}$$

$$2H_2O \rightarrow O_2 + 4H^+ + 4e^- \tag{5}$$

$$2Cl^- \rightarrow Cl_{2(aq)} + 2e^- \tag{6}$$

$$Cl_2 + H_2O \rightarrow ClOH + Cl^- + H^+ \tag{7}$$

For EC, selection of a proper sacrificial AM is critical, since it determines the reactions that take place. Al and Fe electrodes are the most widely used due to their proven reliability and availability (Moussa *et al.* 2017). Initial pH is important because it affects zeta potential and the nature of the released cations. For Al and Fe anodes, the conclusion that maximum performance is attained at a pH range of 5 to 9 has been reached (Gatsios *et al.* 2015; Kobya *et al.* 2016). Current density (i.e. applied current per area of electrode) determines the amount of metal ions released from the anode (Brillas & Martínez-Huitle 2015). The effect of current density on the process efficiency has been reported (Kobya *et al.* 2016). The optimal range of current density strongly depends on the nature of the sample under study, pH and flowrate (Moussa *et al.* 2017). Other factors include conductivity, because at high levels the energy required to carry out the process is reduced. Use of NaCl has been reported to induce the formation of chlorine species that increase process

efficiency (Khandegar & Saroha 2013). NaCl is usually employed to increase wastewater's conductivity. Beside its ionic contribution in carrying the electric charge, it has been found that chloride ions could significantly reduce the adverse effect of other anions such as HCO_3^-, SO_4^{2-}. The addition of NaCl also decreases power consumption because of the increase in conductivity (Brillas & Martínez-Huitle 2015). The number of electro-oxidation cells (NEOC) for EO also affects the process because using multiple cells increases the available area for the electrodes for the oxidation reaction, and the effect of using one or two electrooxidation cells is evaluated in this work.

This work pursues at laboratory scale a coupled EC and EO process in a multi-stage continuous reactor (EC/EO) for treatment of TWW from an industrial facility located in Medellín, Colombia. EC/EO should be capable of removing dissolved and suspended organic pollutants and clarifying the effluents. To achieve this: (i) TWW was characterized for organic matter content (COD, biochemical oxygen demand (BOD$_5$), total organic carbon (TOC)), total solids (*TS*), turbidity, conductivity and biodegradability (BOD$_5$/COD ratio). (ii) The influence on COD removal efficiencies of several factors such as current density, conductivity, AM, pH and the number of electrochemical cells was evaluated for the industrial TWW by EC/EO, using a fractional factorial experimental design. (iii) A Box–Behnken experimental design (BBD) response surface methodology (RSM) was done to determine the optimal operation conditions for achieving maximum DCOD efficiency, taking into account the statistically relevant factors. This optimization is done by simultaneously analyzing all germane factors, taking into account synergistic effects of changing variables couples (i.e. interactions of variables are also considered). (iv) Reproducibility of optimal conditions was assessed. This study deals with industrial TWW and uses a continuous reactor approaching more realistically the scale-up of electrochemical AOPs.

MATERIALS AND METHODS

Materials

TWW was collected from a textile industry from Medellin, Colombia. This facility focuses on the production of denim jeans and generates an average of 800 m³/day of TWW as a result of pre-washing, washing, dyeing and finishing steps where industrial detergents, dyes and other chemical compounds are released as TWW. Samples were kept at 4°C to avoid DCOD during storage, following APHA's standard procedures (APHA 2012). All analytical grade reagents including H_2SO_4 (98%), NaOH pellets (99%) and NaCl (99.5%) were bought from Merck and used as received. All solutions were prepared using ultra-pure water (Milli-Q system; conductivity < 1 μS/cm).

Methods

TWW was characterized for pH, conductivity, absorbance (660 nm), turbidity, TS, COD, TOC, BOD$_5$, BOD$_5$/COD ratio, and generated sludge, using APHA's *Standard Methods* (APHA 2012): (i) a UV-VIS double-beam spectrophotometer equipped with a 1 cm path length quartz cell (Spectronic Genesys 2 PC) was used to measure the absorbance spectra in the range of 200–700 nm; (ii) COD was determined following the closed reflux method with colorimetric determination (method 5220D); (iii) TOC was determined following method 5310D; (iv) BOD$_5$ was determined following the respirometric method (5210B); (v) turbidity was determined with an Orbeco-Hellige turbidimeter (Model 966-01), following 2130B standard method; (vi) APHA's 2540D standard method was employed for TS measurements. Triplicate measurements were performed for all analyses.

Reaction system

A multistage continuous reactor, shown in Figure 1, was used for EC/EO treatment. TWW was fed to the reactor with a Masterflex L/S peristaltic pump model 77521–57 operating at 6.75 mL/min. Sludge formed at the EC cell was collected and characterized by X-ray fluorescence spectroscopy as shown in the supplementary material (available with the online version of this paper) and TWW supernatant with no sludge from the EC cell (i.e. sludge formed precipitates at the EC cell) then fed EO cells to end TWW treatment. A Plexiglas reactor continuously stirred at 60 RPM, with 0.2 L volume and a retention time of 29.63 min, was used for all experiments. The reactor was divided into three compartments with vertical baffles to avoid fluid channeling. The first compartment was used for EC with Fe or Al sacrificial anodes coupled to a titanium cathode. Sludge generated at EC's compartment precipitates while the supernatant flows to EO's cells with no solids. Ti, which has high corrosion resistance, high current efficiency, long working life, high current density, light weight and stable operating voltage, was used to generate active chlorine species for Fe^{2+} oxidation. The subsequent compartments are used for EO with graphite
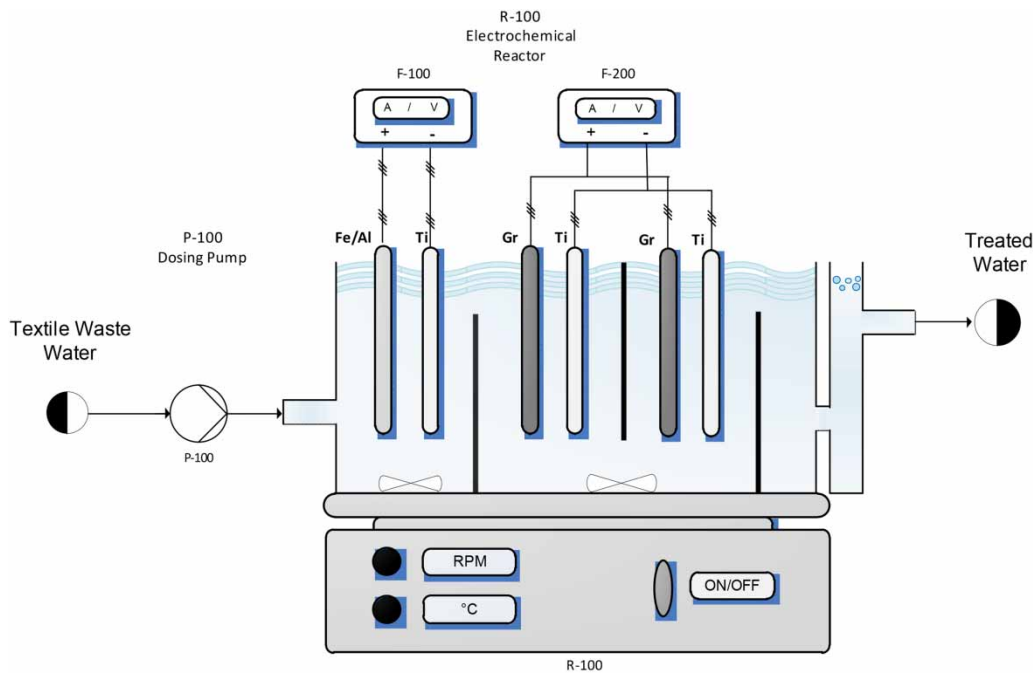
Figure 1 │ Multistage continuous reactor for the application of EC and EO subsequent treatments.

anode and Ti cathodes. All electrodes have dimensions of $4\ cm \times 2.5\ cm \times 0.6\ cm$. Current density for EO was fixed at $10\ mA/cm^2$ for all experiments (according to preliminary tests, not shown here). Bear in mind that the uncoupled EO and EC individual processes could be further optimized by studying the effect of j_{EO}, j_{EC}, pH, and Cd on DCOD for each process. But, when EO is coupled with EC, pH and Cd are the same for both processes and the remaining variables that can be manipulated are j_{EO} and j_{EC}. However, as EC and EO are coupled, one cannot pinpoint how each individual process was affected by the studied factors. The gap between each electrode pair was set at 1 cm. The voltage was regulated with a BK-Precision (Yorba Linda, California) source (0–30 V, 0–5 A). The generated sludge in the EC stage is separated from the surface to a deposit at the end of the reactor, while the treated water flows through a channel at the bottom to be sampled.

Statistical model and experimental design

Two statistical experimental designs were used to systematically evaluate the effect of the operational factors on the process efficiency to remove organic matter presented in the TWW sample. (i) A 2^{5-1} fractional factorial design of experiment was used to establish which factors (i.e. current density ranging between 1 and 5 mA/cm², initial pH ranging

between 4 and 10, conductivity from 3.7 mS/cm up to 5.3 mS/cm, NEOC (one and two cells), and AM (Fe and Al)) affect the most the DCOD process. (ii) A 15 run BBD was done to establish the optimal levels of factors to minimize operating costs (OC) at a desired organic matter DCOD (GilPavas *et al.* 2017) by selecting the three most significant factors detected by the aforementioned fractional factorial design of experiments (i.e. pH, conductivity and current density) and fixing the remaining factors at specific values per cost considerations (i.e. AM was chosen to be iron, and a single electrochemical cell was used). The retention time was 29.63 min. Two replicates were performed for each treatment and the average was reported. When the deviation between both replicates was larger than 4%, both replicates were discarded and the run was repeated. The response variables for the experimental design were COD DCOD (DCOD), calculated with Equation (8), and OC calculated with Equation (9).

$$\%DCOD = \frac{COD_i - COD_t}{COD_i} \times 100 \qquad (8)$$

where COD_i is the initial COD and COD_t is the COD at time t.

$$OC\left(\frac{USD}{m^3}\right) = \frac{1}{V_r}\left(1.08\frac{MIt}{nF} + 2 \times 10^{-4}VIt + 0.2S + 0.027D\right) \qquad (9)$$

where V_r (m^3) is the reaction volume of both EC and EO stages. The first term represents the cost of the anode consumed (USD/kg) per Faraday's law with a safety factor of 20% (i.e. Faraday's law is multiplied by 1.2), where M is the molecular weight (kg/kmol) of anode, I is the electric current (A), t is the retention time (h), n is the amount of electrons transferred, and F is Faraday's constant (26,801.4 Ah/kmol). The second term corresponds to the energy spent in the process with V as the applied voltage (V), S is the amount of NaCl used (kg) and D is the sludge generated (kg). OC is calculated using Colombian official agency of statistics figures from 2017 (i.e., anode's material cost of USD 0.9/kg, energy cost of USD 0.2/kWh, NaCl cost of USD 0.2/kg, and solids disposal cost of USD 27/ton of sludge) in Equation (9).

The percentage of color removal was also measured according to Equation (10).

$$Color\ removal\ (\%) = \frac{(Abs_{i-}Abs_t)}{Abs_i} \times 100 \qquad (10)$$

where Abs_i and Abs_t are the initial absorbance at 660 nm, and absorbance at 660 nm, at time t, respectively.

RSM's BBD results were adjusted to a second-order model as in Equation (11) using Statgraphics Centurion XVI Software:

$$Y_i = \beta_0 + \sum_{i=1}^{3}(\beta_i X_i) + \sum_{i=1}^{3}(\beta_{ii}X_{ii}^2) + \sum_{i=1}^{3}\sum_{j=1}^{3}(\beta_{ij}X_iX_j) \qquad (11)$$

where β_0, β_i, β_{ii}, β_{ij} are the regression coefficients for the intercept, linear, square, and interaction terms, respectively; and X_i and X_j are independent variables. The quality of the model and capacity to estimate experimental results was assessed with the adjusted determination coefficient, R_{adj}^2. Details of this methodology have already been reported before (Ghanbari & Moradi 2015; GilPavas *et al.* 2017). An exhaustive search algorithm using Microsoft Excel VB was used to determine optimum operating conditions that minimize OC while reaching a desired DCOD with the regression models obtained from the analysis of the BBD.

RESULTS AND DISCUSSION

In Table 1 it is possible to see that several physico-chemical parameters of TWW are larger than the permissible limits (e.g. COD, and BOD$_5$/COD ratio). TWW shows an intense blue color mainly due to the presence of indigo dye, which represents a high percentage of the organic compound load. TWW also has a high conductivity due to the presence of different salts. Moreover, TWW has a COD almost twice the permissible COD value limit. This implies that large amounts of non-biodegradable organic matter are present in TWW. In fact, the initial BOD$_5$/COD ratio of 0.19 (< 0.4) indicates that the effluent is not biodegradable (GilPavas *et al.* 2017). Although the legally permissible limit for organic compounds is usually

Table 1 │ Physico-chemical parameters and global operating costs of raw TWW, after EC, and EO steps and after EC/EO combined treatment

Parameter	TWW sample	Permissible limit[a]	After EC process	After EO process	After EC + EO process	Global treatment efficiency (%)
pH	6.92	6–9	5.3	4.5	5.7	–
Conductivity (mS/cm)	3.7	–	4.26	3.81	4.3	–
Absorbance (660 nm)	1.2	–	0.11	0.8	0.05	96%
Turbidity (NTU)	142	–	10	92	7	95%
Total solids (g/L)	4.59	–	2.1	4.25	2.1	54%
Chloride Cl$^-$ (mg/L)	2,026	–	1,950	1,675	1,215	40%
COD (mg O$_2$/L)	702	400	337	540	189	73%
TOC (mg C/L)	225	–	110	177	54	76%
BOD$_5$ (mg O$_2$/L)	132.5	200	87	121	83	37%
BOD$_5$/COD ratio	0.19	0.40	0.26	0.22	0.44	–
Generated sludge (kg/m^3)	–	–	1.3	0	1.3	–
Global operating costs (EC/EO, USD/m^3)	–	–	0.55	0.932	1.47	–

[a]Emission limit values for industrial wastewater discharges into the municipal sewer system according to Res 0631, 17/03/2015, issued by the Ministry of Environment and Sustainable Development, Colombia.

expressed in the terms of COD, in this study the TOC evolution was also monitored.

Preliminary fractional factorial design 2^{5-1}

Experimental conditions evaluated in the preliminary fractional factorial design of the experiment are presented in Table 2 along with the response variable DCOD. DCOD ranged from 8% to 78%. The objective of this set of runs was to find the factors that affect most significantly DCOD by using a Daniel's plot, Figure 2.

Figure 2 displays the Daniel's plot with all effects and interaction alias and a line representing the normal distribution. Effects and interactions falling along the normal distribution line are deemed non-significant, while the remaining are significant. It can be seen that pH and j affect the most DCOD from this analysis, while the remaining factors (AM, Cd and NEOC) are not significant. A correlation analysis between all variables from the fractional factorial design of experiment is also performed to complement the analysis provided by Daniel's plot and prevent the exclusion of any relevant factor in the Box–Behnken design. The correlation coefficients of DCOD with j of 0.798, with pH of -0.564 and with Cd of -0.114, show a strong dependence of DCOD with j, and pH and a mild
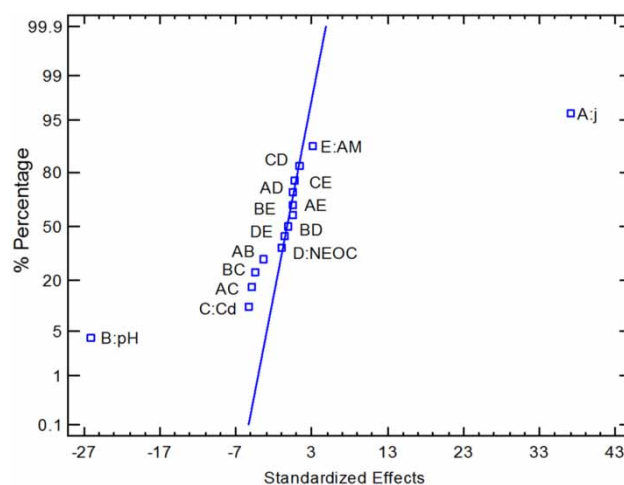

Figure 2 | Daniel's plot for the 2^{5-1} fractional factorial design of experiment on DCOD.

dependency on Cd. Neither AM nor NEOC are significantly correlated to DCOD (i.e. -0.021 and -0.067 respectively).

AM and NEOC effects

Different studies have indicated that aluminum is a more suitable AM than iron to perform EC because it releases Al^{3+} cations, which are more effective in destabilizing pollutants than Fe^{2+} cations released from iron electrodes (Moussa et al. 2017). However, in Daniel's plot, AM falls along the normal distribution line, implying that this is not a significant factor. This is further evidenced by a t-test that leads to the conclusion that there are no significant differences in DCOD caused by AM (i.e. a p-value of 0.8 indicates that the null hypothesis of equal means cannot be rejected). Iron electrodes are reported to present good performances especially when oxidizing agents, such as oxygen, are present in sufficient amount to convert all Fe^{2+} to Fe^{3+} (Hakizimana et al. 2017). The oxidation of Fe^{2+} to Fe^{3+} depends strongly on the pH and dissolved oxygen concentration. In acid media, Fe^{2+} cations oxidize very slowly in contact with dissolved oxygen, while in neutral or alkaline media Fe^{2+} is immediately transformed into $Fe(OH)_2$ which is quickly oxidized by dissolved oxygen to $Fe(OH)_3$. Active chlorine species (i.e. Cl_2, HOCl and OCl^-) are also capable of oxidizing Fe^{2+} to Fe^{3+}. Also, as current density increases, anodic dissolution is favored so that metallic sludge residues increase. Moreover, the amount of sludge increases with operating time. In textile industries, oxidizing agents, such as potassium permanganate, are used to decolorize and bleach fabrics. Also, a high concentration of chloride ions induces the

Table 2 | Experimental results for preliminary fractional design 2^{5-1}

Experimental conditions

J (mA/cm²)	pH	Cd (mS/cm)	NEOC	AM	Response variable (%) DCOD
1	10	5.3	1	Fe	12.24
1	10	3.7	2	Fe	14.24
1	10	3.7	1	Al	14.85
5	10	5.3	1	Al	35.51
1	10	5.3	2	Al	8.11
1	4	5.3	2	Fe	38.44
5	4	3.7	2	Fe	78.45
5	10	5.3	2	Fe	41.25
1	4	3.7	1	Fe	35.48
5	4	3.7	1	Al	77.9
1	4	5.3	1	Al	35.48
5	4	5.3	1	Fe	74.48
5	10	3.7	2	Al	51.17
1	4	3.7	2	Al	31.15
5	4	5.3	2	Al	71.5
5	10	3.7	1	Fe	56.14

electrochemical formation of active chlorine in the EC and EO cells. Therefore, the presence of these oxidants improves the transition of Fe^{2+} to Fe^{3+}, making iron a suitable AM to perform the process. Another advantage of iron is that its cost is lower than that of aluminum. The specific drawback of EC is the need for sludge handling, but chemical coagulation and the activated sludge process have to address the same issue. From these considerations, iron was chosen for the next RSM's Box–Behnken design of experiment. *NEOC*'s non-departure from the normal probability line in Daniel's plot indicates that the number of electrochemical cells is not significant for DCOD. EO process effectiveness is related to current density and retention time. Three reasons are hypothesized for the non-significance of NEOC: (1) retention time is not large enough to detect a significant change in DCOD, (2) current density is relatively low (10 mA/cm^2) to be able to increase process efficiency and (3) electrode's area change is not large enough to produce a significant change in DCOD. Therefore, a single electrooxidation cell was used in the subsequent Box–Behnken design of experiment.

Conductivity effect (Cd)

Despite not being detected as a significant factor by Daniel's plot, increasing conductivity reduces the energy required to carry out the process (Khandegar & Saroha 2013). Therefore, we deem it important to include Cd in the BBD that also considers OC as a response variable. It can also be seen that despite not being detected as a significant factor in Daniel's plot in Figure 2, Cd is the third most correlated factor with DCOD and its inclusion as a third variable with j and pH in the BBD, is also justified statistically.

pH effect

It can be seen that *pH* presents a large departure from the normal distribution line Daniel's plot in Figure 2. Therefore, this factor is statistically significant on DCOD. Lower pH values result in increased DCOD, while higher values in lower DCOD. These results differ from other reports, when pH greater than 5 resulted in better coagulation or EC because at lower pH metal hydroxides, responsible for the precipitation of pollutants, are not formed (Gatsios *et al.* 2015); however, using EC simultaneously with EO can explain the discrepancy; also, the nature of the pollutant influences the coagulation efficiency. A different study of wastewater containing indigo dye showed that using a ferric salt coagulation was enhanced near acid *pH* (GilPavas

et al. 2017). As pH is significant, it is evaluated at a wider range between 4 and 10 (i.e. in acid, neutral and alkaline conditions) in the forthcoming BBD. On the other hand, the action of active chlorine species in EO treatment with graphite is dependent on the solution pH. At a pH ca. 4.0, Cl_3^- is formed in very low concentration, whereas at a pH near 3.0, the predominant species is $Cl_2(aq)$. Meanwhile, the prevalent species at a pH range of 3–8 and for pH > 8.0 are HClO and ClO^-, respectively. Then, Cl^- mediated oxidation of dyes with these species is expected to be faster in acid media than in alkaline media because of the higher standard potential of $Cl_2(aq)$ ($E° = 1.36$ V/SHE) and HClO ($E° = 1.49$ V/SHE) than ClO^- ($E° = 0.89$ V/SHE).

Current density effect (j)

According to Daniel's plot in Figure 2, EC's current density (j) is the most significant factor on DCOD from its departure from the normal distribution line. This is also confirmed by the high correlation between DCOD and j for the fractional factorial design. j determines the coagulant dosage at the anode and the hydrogen gas (H_2) evolution at the cathode governed by Faraday's law (Hakizimana *et al.* 2017). A high level of j implies a fast consumption of the sacrificial electrodes and a high-energy cost associated with the voltage required to conduct the process, therefore, this factor is considered for the subsequent BBD experimental design, where the operational costs are also taken into consideration in the optimization analysis.

RSM Box–Behnken design of experiment optimization

The experimental conditions and response variables (DCOD) and OC are presented in Table 3. DCOD varied between 6 and 73% while OC varied from 1.03 to USD 1.60/m^3. Both DCOD and OC data were adjusted to second order polynomial models to determine the operating conditions that maximize DCOD at the least possible OC.

Multivariable non-linear regression modelling

The results for the multivariable regressions for OC and DCOD are shown in Table 4. It can be seen, by examining p-values, that there are some factors and interactions that are not significant within a 95% confidence interval (i.e. $p > 0.05$) for the estimated parameter (i.e. β_i). For OC, the factors j, Cd and pH, the interaction j:Cd and the quadratic terms j^2 and Cd^2 are significant. The remaining interactions and pH quadratic term are not significant for

Table 3 | Experimental and predicted results of the DCOD and the OC according to the BBD

	Experimental conditions			Response variables			
				DCOD (%)		OC (USD/m³)	
Run	pH	Cd (mS/cm)	j_{EC} (mA/cm²)	$Y_{exp.}$	$Y_{pred.}$	$Y_{exp.}$	$Y_{pred.}$
1	7	4.5	3	34.12	34.53	1.31	1.31
2	10	3.7	3	25.22	29.33	1.29	1.3
3	7	5.3	1	23.08	25.18	1.03	1.03
4	7	5.3	5	59.24	57.96	1.51	1.51
5	10	4.5	1	6.55	1.16	1.07	1.07
6	4	5.3	3	57.26	53.15	1.27	1.27
7	4	4.5	1	25.93	27.94	1.09	1.1
8	7	3.7	5	73.5	71.4	1.59	1.59
9	7	3.7	1	22.65	23.93	1.06	1.06
10	4	3.7	3	60.11	56.82	1.32	1.32
11	10	5.3	3	17.52	20.81	1.24	1.24
12	10	4.5	5	40.17	38.16	1.59	1.58
13	7	4.5	3	35	34.53	1.31	1.31
14	7	4.5	3	34.47	34.53	1.31	1.31
15	4	4.5	5	65.81	71.2	1.6	1.6

Iron was used as anode material ($AM = Fe$) and a single electrooxidation cell was used ($NEOC = 1$).
Y_{exp}: Experimental results, Y_{pred}: Predicted results by regression models.

OC. For DCOD, the factors j and pH, and the quadratic term Cd^2 are significant. None of the other factors, quadratic terms and interactions are significant for DCOD. Adequacy F-test for both response variables indicates that at least one of the factors, interactions or quadratic terms is different from zero and that both models are useful. This is further evidenced by the overall p-value reported for both regressions, which is much lower than 0.05 in both cases. The quality of fit of both models is very good, as evidenced by the multiple determination coefficient: $R^2 = 0.9758$ for DCOD and $R^2 = 0.9997$ for OC. The adjusted multiple correlation coefficient changed marginally with respect to the multiple determination coefficient for both DCOD and OC, indicating that there were enough data points to conclude soundly about the quality of fit. Also, predicted values by regression models and experimental values agree very well, as shown in Table 3.

The models for DCOD and OC, as in Table 3, are shown in Equations (12) and (13).

$$DCOD = 242.31 + 1.57^*pH - 102.37^*Cd + 18.68^*j$$
$$- 0.25^*pH^2 - 0.505^*pH^*Cd - 0.26^*pH^*j$$
$$+ 12.11^*Cd^2 - 2.295^*Cd^*j + 0.584^*j^2 \quad (12)$$

Table 4 | Results for the multivariable regressions for OC and DCOD

	Response variable: DCOD					Response variable: OC				
Parameter	Estimate	Std. error	t value	Pr(>|t|)	p-value	Estimate	Std. error	t value	Pr(>|t|)	p-value
(Intercept)	−0.03	0.110	0.26	0.83	–	242.307	96.523	2.51	0.054	
pH	−0.01	0.075	−1.7	0.15	0.0004	1.574	6.574	0.24	0.82	0.0030
j	0.13	0.010	12	6.10×10^{-5}	0.0001	18.68	8.909	2.097	0.09	0.000
Cd	0.48	0.045	11	1.20×10^{-4}	0.157	−102.371	39.023	−2.623	0.047	0.0001
pH:j	4.2×10^{-4}	4.9×10^{-4}	0.85	0.44	0.572	−0.261	0.432	−0.604	0.572	0.4366
pH:Cd	4.1×10^{-18}	1.2×10^{-3}	0	1.00	0.6594	−0.505	1.079	−0.468	0.659	1
j:Cd	-7.8×10^{-3}	1.9×10^{-3}	−4.2	0.01	0.2154	−2.295	1.619	−1.418	0.215	0.0083
pH^2	5.6×10^{-4}	3.4×10^{-4}	1.6	0.17	0.4415	−0.25	0.3	−0.836	0.441	0.1653
j^2	5.6×10^{-3}	7.7×10^{-4}	7.3	7.50×10^{-4}	0.4255	0.584	0.674	0.867	0.426	0.0008
Cd^2	−0.06	4.8×10^{-3}	−11	9.20×10^{-5}	0.0348	12.109	4.212	2.875	0.035	0.0001
Multiple R^2: 0.9758						Multiple R^2: 0.9997				
Adjusted R^2: 0.9324						Adjusted R^2: 0.9991				
F-statistic: 22.45 on 9 and 5 DF.						F-statistic: 1,696 on 9 and 5 DF.				
p-value: 0.0016						p-value: 3.6×10^{-8}				

$$OC = -0.0249 - 0.01278^*\text{pH} + 0.482^*\text{Cd} + 0.126^*j$$
$$- 0.00055^*\text{pH}^2 + 0.00042^*\text{pH}^*j - 0.0546^*\text{Cd}^2$$
$$- 0.0078^*\text{Cd}^*j + 0.0056^*j^2 \qquad (13)$$

Process optimization

To determine the minimum attainable OC to achieve a DCOD higher than a specific desired value, the optimization problem depicted in Equation (14) coupled with Equations (12) and (13) was solved by using Microsoft Excel's solver.

$$\min OC(\text{pH}, j, \text{Cd})$$
$$s.t.$$
$$\text{DCOD} \geq 70\ \% $$
$$4 \leq \text{pH} \leq 10 \qquad (14)$$
$$3.7 \leq \text{Cd} \leq 5.3$$
$$1 \leq j \leq 5$$

This optimization problem is non-linear convex in a convex region which leads to the inference that an overall global minimum exists within the restrictions. However, as the objective function for the operating cost OC (pH, Cd, j) is flat near its minimum value and OC is discrete (because the minimum dollar denomination is USD 0.01), multiple optimum values are detected.

This optimization problem, solved using different initial guesses for pH, Cd and j, converged in the vast majority of

the cases to pH = 4 and Cd = 3.7 mS/cm. When varying j from 4 to 4.3 mA/cm², at pH = 4 and Cd = 3.7 mS/cm, OC changes are marginal from USD 1.46/m³ to USD 1.50/m³ respectively. Therefore, pH = 4, Cd = 3.7 mS/cm and j = 4.1 mA/cm² are chosen to attain DCOD of 71.44% and OC of USD 1.47/m³ because it is necessary to operate at a high current density (j) to increase DCOD. Notice also that at these conditions there is no cost for conductivity adjustment, implying that energy consumption reduction is not significant compared to the cost of NaCl and, therefore, it is preferable to operate at TWW's natural conductivity. As for pH, low pH is better for the EC/EO combined process, and the cost of H_2SO_4 required to adjust pH is low compared to the energy cost.

Model validation and individual process contributions

In order to validate the capacity of the model to correctly predict DCOD and the stability of the process with time, the output of the reactor was monitored during 90 minutes at the optimum conditions of pH = 4, Cd = 3.7 mS/cm and j = 4.1 mA/cm² to yield DCOD of 71.44% and OC of USD 1.47/m³. Also, individual stages of EC and EO processes were evaluated to determine their individual contributions to DCOD. Figure 3 shows that the coupled EC/EO continuous process stabilized at around DCOD of 72%, agreeing with the predicted value of 71.44% within experimental error. EC process contributes more to DCOD than EO (i.e. after EC, *DCOD* is 51%). It can also be seen that DCOD increases with time until 30 min, when DCOD
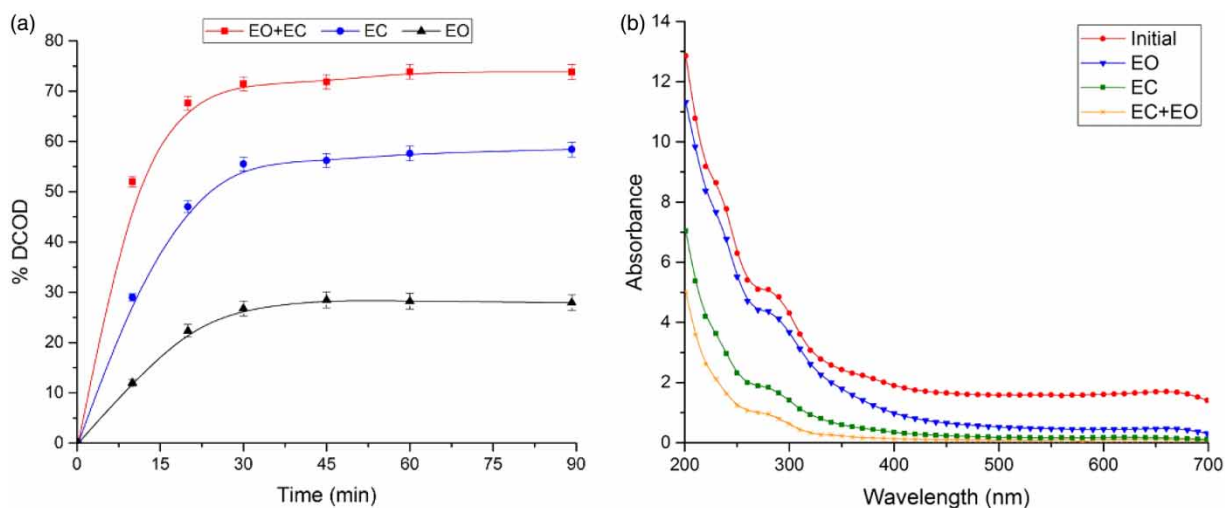

Figure 3 │ (a) Validation of the regression models and individual contributions of EC (pH:4. Cd: 3.7 mS/cm and j: 4.1 mA/cm²), EO (pH:4. Cd: 3.7 mS/cm and j: 10 mA/cm²) and EC/EO (pH:4. Cd: 3.7 mS/cm, j_EC: 4.1 mA/cm² and j_EO: 10 mA/cm²) on DCOD, (b) UV-VIS absorption spectra.

levels off. This leads to the conclusion that the retention time should be studied in future research as it is a very relevant variable. These results can be explained by TWW's main pollutant (indigo dye), which is insoluble in water but remains suspended due to the effect of chemical additives used in the process. EC works by suspended solids destabilization and, therefore, it is highly efficient in removing indigo (Tezcan & Aytac 2013). On the other hand, EO's mechanism is explained by the chemical oxidation of the pollutants with hydroxyl radicals formed at the electrodes, where this type of reaction is more efficient with soluble compounds (e.g. detergents present at low concentrations). The combination of EC/EO is able to obtain a high level of organic matter removal. However, in order to obtain efficiencies near 100%, conditions involving higher operational cost would be needed.

In addition to DCOD, other TWW's physico-chemical parameters changed after EC/EO. Table 1 shows the physico-chemical properties of TWW before and after the EC. After EC/EO, total organic carbon (TOC) is reduced by 76% while BOD_5 (BOD) is reduced by 73%, implying that EC is efficient in removing a high content of organics. Turbidity removal was 95%, meaning that almost all suspended solids are removed from water by EC and that the remaining pollutants are soluble organic compounds that would require a more energy intensive EO stage to be completely removed. TS are reduced by 54%. Also, in Table 1, BOD_5/COD of raw wastewater is 0.19, indicating that the biodegradability of this wastewater is very low. BOD_5/COD value increased to 0.44 after EC/EO processes. pH of treated TWW is substantially reduced so that further adjustment is necessary before discharge. As can be seen in Figure 3(b), before treatment ($t = 0$ min), the UV-vis spectrum consists of two main characteristic absorption bands: at 290 nm, assigned to benzenic rings; and at 660 nm, assigned to indigo dye. After 30 min of reaction, the band at 660 nm disappeared and the color of the solution was completely degraded. However, the other band at 290 nm remains, and aromatic compounds removal is ca. 84.3%, indicating that some intermediate DCOD compounds are formed.

TWW treatment costs have been reported in the literature (Brillas & Martínez-Huitle 2015; Kobya et al. 2016; GilPavas et al. 2017; Soares et al. 2017) ranging from USD 0.50/m^3 to USD 14.50/m^3. Bear in mind that most research is done in different countries with costs for energy, electrodes, etc. that are vastly different and not all reported TWW treatment processes yield the same efficiency for DCOD, TOC, BOD, etc. While comparing OC between studies is inexact, we deem that OC reported in this study is realistic and modest (USD 1.47/m^3).

CONCLUSIONS

In this study, TWW from the fabrication of denim was treated using a multistage EC/EO continuous reactor. TWW contained a high load of organic compounds represented in a COD of 702 mg/L and a TOC of 225 mg/L, a total amount of solids of 4.59 g/L with a turbidity of 142 NTU and a low biodegradability ratio BOD_5/COD of 0.19, unfit to be treated by biological based treatments. DCOD kinetics of TOC remain to be studied in future works. The main conclusions obtained from experimental results are as follows:

- Iron or aluminum sacrificial anodes present similar performance efficiencies in the EC stage; since aluminum is more expensive than iron, the latter is selected as the best electrode material to carry out the process.
- Optimum operating conditions to achieve a DCOD of 71.44% at a minimum OC of US $1.47/m^3 were pH = 4, Cd = 3.7 mS/cm and $j = 4.1$ mA/cm^2. Validation of the selected conditions showed that the efficiency of the process was stable during 90 minutes of operation.
- Individual contribution to DCOD from EC and EO showed that EC alone resulted in DCOD of 51%, while EO contributed with 21% of DCOD. The larger contribution of EC is explained by the large amount of suspended solids in TWW (mainly indigo dye).
- Combined EC/EO increased TWW's treatment efficiency because color removal was near 100%, DCOD was larger than 70%, TOC's reduction was larger than 60%, and biodegradability increased to a BOD_5/COD ratio of 0.44 at an OC of USD 1.47/m^3.

This study showed the potential of a continuous multistage EC/EO reaction system for the treatment of industrial wash water resulting from the denim wash manufacturing processes. It can be concluded that the integrated technology is a suitable alternative for industrial TWWs.

ACKNOWLEDGEMENTS

REFERENCES

Alinsafi, A., Khemis, M., Pons, M. N., Leclerc, J. P., Yaacoubi, A., Benhammouc, A. & Nejmeddine, A. 2005 Electro-coagulation of reactive textile dyes and textile wastewater. *Chemical Engineering and Processing* **44**, 461–470.

Amor, C., Torres-Socías, J. A. P., Maldonado, M. I., Oller, I., Malato, S. y. & Lucas, M. S. 2015 Mature landfill leachate treatment by coagulation-flocculation combined with Fenton and solar photo-Fenton processes. *Journal of Hazardous Materials* **286**, 261–268.

APHA 2012 *Standard Methods for the Examination of Water and Wastewater*. 22nd edn. American Public Health Association, Washington.

Brillas, E. & Martínez-Huitle, C. A. 2015 Decontamination of wastewaters containing synthetic organic dyes by electrochemical methods: an updated review. *Applied Catalysis B: Environmental* **166–167**, 603–643.

Gatsios, E., Hahladakis, J. N. & Gidarakos, E. 2015 Optimization of electrocoagulation (EC) process for the purification of a real industrial wastewater from toxic metals. *Journal of Environmental Management* **154**, 117–127.

Ghanbari, F. & Moradi, M. 2015 A comparative study of electrocoagulation, electrochemical Fenton, electro-Fenton and peroxi-coagulation for decolorization of real textile wastewater: electrical energy consumption and biodegradability improvement. *Journal of Environmental Chemical Engineering* **3**, 499–506.

GilPavas, E., Dobrosz-Gómez, I. & Gómez-García, M. A. 2017 Coagulation-flocculation sequential with Fenton or photo-Fenton processes as an alternative for the industrial textile wastewater treatment. *Journal of Environmental Management* **191**, 189–197.

Hakizimana, J. N., Gourich, B., Chafi, M., Stiriba, Y., Vial, C., Drogui, P. & Naja, J. 2017 Electrocoagulation process in water treatment: a review of electrocoagulation modeling approaches. *Desalination* **404**, 1–21.

Kariyajjanavar, P., Narayana, J. & Nayaka, Y. A. 2013 Degradation of textile dye C.I. Vat Black 27 by electrochemical method by using carbon electrodes. *Journal of Environmental Chemical Engineering* **1**, 975–980.

Khandegar, V. & Saroha, A. K. 2013 Electrocoagulation for the treatment of textile industry effluent – a review. *Journal Environmental Management* **128**, 949–963.

Kobya, M., Gengec, E. & Demirbas, E. 2016 Operating parameters and costs assessments of a real dyehouse wastewater effluent treated by a continuous electrocoagulation process. *Chemical Engineering and Processing: Process Intensification* **101**, 87–100.

Moreira, F. C., Boaventura, R. A. R., Brillas, E. & Vilar, V. J. P. 2017 Electrochemical advanced oxidation processes: a review on their application to synthetic and real wastewaters. *Applied Catalysis B: Environmental* **202**, 217–261.

Moussa, D. T., El-Naas, M. H., Nasser, M. & Al-Marri, M. J. 2017 A comprehensive review of electrocoagulation for water treatment: potentials and challenges. *Journal of Environmental Management* **186**, 24–41.

Phalakornkule, C., Polgumhang, S., Tongdaung, W., Karakat, B. & Nuyut, T. 2010 Electrocoagulation of blue reactive, red disperse and mixed dyes, and application in treating textile effluent. *Journal of Environmental Management* **91**, 918–926.

Rodrigues, C. S. D., Neto, A. R., Duda, R. M., Oliveira, R. A., Boaventura, R. A. R. & Madeira, L. M. 2017 Combination of chemical coagulation, photo-Fenton oxidation and biodegradation for the treatment of vinasse from sugar cane ethanol distillery. *Journal of Cleaner Production* **142**, 3634–3644.

Soares, P. A., Souza, R., Soler, J., Silva, T. F., Guelli, S., Boaventura, R. A. R. & Vilar, V. J. P. 2017 Remediation of a synthetic textile wastewater from polyester-cotton dyeing combining biological and photochemical oxidation processes. *Separation and Purification Technology* **172**, 450–462.

Sreeja, P. H. & Sosamony, K. J. 2016 A comparative study of homogeneous and heterogeneous photo-Fenton process for textile wastewater treatment. *Procedia Technology* **24**, 217–223.

Tezcan, U. & Aytac, E. 2013 Electrocoagulation in a packed bed reactor-complete treatment of color and cod from real textile wastewater. *Journal of Environmental Management* **123**, 113–119.

Verma, A. K., Dash, R. R. & Bhunia, P. 2012 A review on chemical coagulation/flocculation technologies for removal of colour from textile wastewaters. *Journal of Environmental Management* **93**, 154–168.